Unresolved spatial variability and microphysical process rates in large-scale models

Robert Pincus

Cooperative Institute for Meteorological Satellite Studies, University of Wisconsin, Madison

Stephen A. Klein

NOAA Geophysical Fluid Dynamics Laboratory, Princeton University, Princeton, New Jersey

Abstract. Prognostic cloud schemes in large-scale models are typically formulated in terms of grid-cell average values of cloud condensate concentration q, although variability in q at spatial scales smaller than the grid cell is known to exist. Because the source and sink processes modifying q are nonlinear, the process rates computed using the mean value of q are biased relative to process rates which account for subgrid-scale variability. A preliminary assessment shows that these biases can modify instantaneous process rates by as much as a factor of 2. Observations of q at a continental site suggest that the bias is avoided in current practice through the arbitrary tuning of model parameters. Models might be improved if subgrid-scale variability in q were explicitly considered; several approaches to this goal are suggested.

1. Introduction: Linear Averaging of Nonlinear Process Rates

The representation of clouds in large-scale atmospheric models has become substantially more realistic in the past decade with the introduction of prognostic cloud schemes [e.g., *Sundquist*, 1978; *Tiedtke*, 1993; *Del Genio et al.*, 1996; *Fowler et al.*, 1996; *Rotstayn*, 1997; *Rasch and Kristjánsson*, 1998]. These schemes explicitly compute the average concentrations of water and ice in the cloudy portion of each grid cell as a time-evolving balance between sources and sinks of cloud water and ice. Large-scale dynamics, the hydrologic cycle, and cloud radiative properties are related in the natural world; basing these links on physical processes rather than diagnostic relationships in models should allow for more accurate representation of the mean climate and its sensitivity to change.

Prognostic cloud schemes, like nearly all components of a large-scale model, are formulated in terms of average values within the grid cell. In nature, though, the concentration q of cloud water and ice varies at spatial scales from the planetary to the centimeter [*Tjemkes and Visser*, 1994; *Davis et al.*, 1999]. When q is represented solely by its average in some volume, any variability within that domain is effectively ignored. Larger domains typically encompass more diverse values of q, so the spatial resolution of the model (i.e., the averaging scale) affects how much variability within each grid cell is neglected. Grid spacings in large-scale models (LSMs) of the atmosphere currently range from about 50 km in numerical weather prediction models to 250 km or greater in climate simulation models; at the latter grid size the neglected variability can be a substantial fraction of the mean value.

Some amount of subgrid-scale variability is already accounted for in large-scale models. Most either diagnose or make a prediction of the volume within each grid cell occupied by clouds. Grid cell mean process rates are then computed as the product of this

cloud fraction and the process rate computed from the in-cloud value of q. The cloudy portion of the grid cell is further divided into stratiform regions with weak vertical velocities and convective regions with more vigorous vertical motion. Microphysical process rates are computed separately for the stratiform and (presumably much smaller) convective regions. Both the cloudy/clear and stratiform/convective distinctions are somewhat arbitrary approximations to the underlying variability.

One well-known impact of unresolved spatial variability in climate simulations is a systematic bias in calculations of cloud reflectance [*Cahalan et al.*, 1994]. Because albedo is a convex function of cloud optical thickness τ, a constant change in τ causes larger changes in albedo in optically thin clouds than in optically thick clouds. This nonlinearity means that a domain containing any variability in optical thickness will always be less reflective, on average, than the same domain filled with uniform clouds of the mean optical thickness. This plane parallel homogeneous (PPH) bias is potentially serious in climate simulations, where biases in albedo and the amount of absorbed solar radiation must be compensated for by changes in other portions of the energy budget.

But radiation is only one of many nonlinear processes acting in a large-scale model. In any process that depends nonlinearly on a spatially variable physical quantity, the presence of subgrid-scale variability causes a bias between the average of the process rate over the grid cell and the process rate computed from the grid cell average.

This paper provides an initial assessment of the impact of subgrid-scale variability on the magnitude of instantaneous process rates in prognostic cloud schemes. We focus on the bias that results from assuming a single value of q in the portion of the grid cell filled with stratiform clouds. We describe how process rates are biased in the presence of subgrid-scale variability in q, show how this bias may be evaluated, and assess the magnitude of the bias for a variety of example distributions. We demonstrate that the presence of subgrid-scale variability is a significant factor driving the need to arbitrarily tune large-scale model parameters. We close by enumerating some of the issues that will require attention if a treatment of subgrid-scale variability is to be incorporated into large-scale models.

Our intent here is to provide a framework for discussion and fuel for debate. The examples in this paper, therefore, are an attempt to balance realism and simplicity, but are not meant as exhaustive calculations of the impact's magnitude.

2. Computing Process Rates for Distributions of Cloud Water Concentration

2.1. Computing Domain Averaged Process Rates

In large-scale models the local rate of change of water and ice concentration is determined by accounting for every process acting within the grid cell, each of which proceeds at its own rate R. Linking process rates to local cloud properties and thermodynamic state is the heart of parameterization; these relationships are developed using some combination of observations and the results of more detailed models. Although microphysical processes may in reality depend on aspects of the drop size distribution, this information is not available in most LSMs. We therefore focus on bulk schemes in which the source and sink rates for cloud condensate are parameterized in terms of q itself ($R = R(q)$). We refer to schemes in which R is a function of the mean value $\bar{q}$ within the grid cell alone as single-value parameterization schemes.

In the presence of subgrid-scale variability the average process rate $\overline{R(q)}$ within a model grid cell is obtained by integrating the process rate across the domain. Cloud physical processes are most often local; the condensation rate at one location, for example, does not depend on cloud properties at any other location. Integration over the spatial domain is therefore equivalent to integration over the probability distribution function (PDF) of condensate concentration $P(q)$. The relative bias between the average process rate and the process rate computed from the average value of q is then

$$B = \frac{\overline{R(q)} - R(\bar{q})}{R(\bar{q})} = \frac{\int_0^\infty P(q)R(q)dq}{R(\bar{q})} - 1 . \quad (1)$$

The domain average process rate can be recovered from the single-value process rate and (1) as

$$\overline{R(q)} = (1 + B)R(\bar{q}) . \quad (2)$$

Average process rates are overestimated by single value schemes ($B < 0$) where $d^2R(q)/dq^2 < 0$ and underestimated where this derivative is greater then 0; the bias vanishes when the process rate is linear in q or if the rate does not depend on q. The size of the bias in general depends on the amount of nonlinearity and on the shape of $P(q)$. Making an analogy to the PPH bias, we refer to B as the "subgrid-scale homogeneity" (SSH) bias.

The dependence of process rates R on q takes many mathematical forms in large-scale models; for the sake of illustration we examine processes rates that are parameterized as $R \sim q^n$. For processes such as autoconversion, n may reach 7/3 [*Manton and Cotton*, 1977; *Khairoutdinov and Kogan*, 2000] or higher [*Beheng*, 1994]. Rates computed for any $P(q)$ will be greater than the rate computed with $\bar{q}$ when $n > 1$ regardless of the details of the distribution. We refer to schemes which compute process rates by integrating over the PDF as distribution-based schemes.

2.2. Describing Subgrid-Scale Variability in Cloud Condensate

Evaluation of (1) requires knowledge of $P(q)$ within each model grid cell. What distributions might be reasonable? The true PDFs of cloud condensate within LSM grid cell-sized domains are not known and almost certainly depend on many aspects of the atmospheric state. We therefore seek reasonable example distribu-

tions that we can use to assess the order of magnitude of the SSH bias.

We partition the variability of q within each grid cell into horizontal and vertical components [*Considine et al.*, 1997]. We assume for simplicity that q varies linearly with height with slope β, which may be positive or negative. We represent horizontal variability using two-parameter analytic distributions. One parameter is typically related to the mean value of the PDF, while a second controls the width of the distribution. The three-dimensional PDF of q within each grid cell is then defined by the two parameters of the horizontal distribution and the value of β.

How can we estimate appropriate parameter values for $P(q)$? No instrument exists to measure the instantaneous three-dimensional distribution of q within a large domain. We rely instead on observations of τ made by imaging satellite radiometers, which we use in conjunction with physical assumptions to obtain a rough proxy for q. In marine boundary layer clouds, populations of τ in domains about the size of LSM grid cells are well represented by a gamma distribution [*Barker et al.*, 1996; *Pincus et al.*, 1999]

$$P(\tau) = \frac{\nu}{\bar{\tau}}\frac{1}{\Gamma(\nu)}\tau^{\nu-1}\exp\left(-\frac{\nu\tau}{\bar{\tau}}\right), \quad (3)$$

where Γ is the Euler gamma function. The average value of this distribution is $\bar{\tau}$; the width of the distribution increases as the shape parameter ν decreases.

3. Assessing the Impact of Subgrid-Scale Variability

Our prototype distributions of cloud condensate concentration may now be combined with the assumed dependence of process rate on q to obtain a rough estimate of the magnitude of the SSH bias. The examples in this section are meant to be illustrative as well as quantitative, so we proceed from simple computations to complex ones.

3.1. The Effects of Vertical Stratification: Uniform Distributions of Water Content

Consider first a horizontally uniform but vertically stratified cloud which exactly fills a model grid cell of height Δz. The average value of q is the value at the geometric midpoint of the grid cell. The PDF is constant between 0 and $\max(q) = 2\bar{q}$; normalization requires that $P(q) = 1/2\bar{q}$. We compute the SSH bias using (1) as

$$B = \left(\frac{1}{2\bar{q}}\int_0^{2\bar{q}} q^n dq\right)\Big/\bar{q}^n - 1$$

$$= \frac{2^n}{n+1} - 1. \quad (4)$$

Because the distribution of q is uniform, the magnitude of this error (shown as a dashed line in Figure 1) depends only on the degree of nonlinearity of the process rate. Average process rates are overestimated by a modest 7% at $n = 1/2$ and underestimated by about 50% at $n = 7/3$.

The SSH bias computed with (1) applies when the process occurs everywhere within the model grid cell or, equivalently, at all values of q. Some processes, however, occur only when a quantity has exceeded a threshold value. Autoconversion, for example, does not occur until cloud drops are large enough to fall past one another with appreciable speed. This change in behavior is often represented in LSMs by setting autoconversion rates to zero until some threshold value of drop size (as inferred from q) is reached,
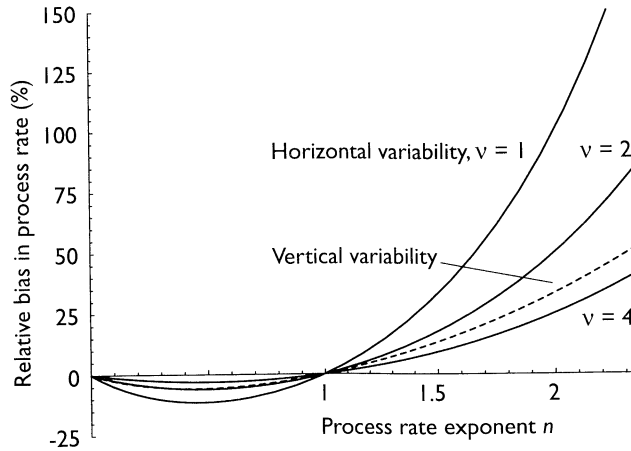
Figure 1. Bias in the domain-averaged rate of a microphysical process R in the presence of variability in condensate concentration q. The process rate is proportional to q^n; values of n far from 1 indicate strongly nonlinear processes. The bias due to linear vertical variation of q with height (shown as a dashed line) depends only on the degree of nonlinearity of the process. Horizontal variability is modeled as a gamma distribution in which variability decreases with shape parameter v; the bias is shown for values of $v = 1, 2$, and 4. Instantaneous estimates of process rate are affected strongly when the process is highly nonlinear.

then allowing the process rate to vary with q [*Rotstayn*, 1997]. A single-value scheme exhibits binary behavior: process rates change abruptly from zero to a finite value as q passes through the threshold value q_0. When $\bar{q} > q_0$ the SSH bias can be computed using (1) with the lower bound in the integral set to q_0:

$$B = \frac{2^n}{n+1} - \frac{(q_0/\bar{q})^{n+1}}{2(n+1)} - 1. \tag{5}$$

When $\bar{q} < q_0$, single-value schemes indicate that the process is not active at all. When vertical stratification is taken into account, however, q may exceed q_0 in denser parts of the cloud [*Rotstayn*, 2000]. Thus distribution based schemes may predict small but finite process rates when a single-value scheme predicts none even if both schemes use the same threshold. Under these circumstances, (1) is undefined but the process rate itself varies smoothly with q. Schemes which account for vertical variability in q, therefore, predict smooth changes in process rates even for threshold-based processes.

3.2. The Impact of Horizontal Variability

Imagine next a cloud which is vertically uniform but exhibits horizontal variability in optical thickness τ, and assume that the distribution of q follows that of τ. For an optical depth population described by a gamma distribution as in (3), the SSH bias is

$$B = \frac{1}{v^n} \frac{\Gamma(n+v)}{\Gamma(v)}. \tag{6}$$

This bias depends on both the amount of nonlinearity in the process rate and on the amount of spatial variability within the model grid cell (see Figure 1). When the standard deviation of the distribution is about 60% of the mean value ($v = (\bar{\tau}/\sigma)^2 = 3$, not shown), the bias due to horizontal variability alone almost exactly matches the bias due to vertical variability (dashed line).

We have seen that parts of the PDF may exceed a given threshold value q_0 when q within the grid cell is distributed about its

mean value. For processes including a threshold value, (1) can be evaluated only when $\bar{q} > q_0$, when its value is

$$B = \frac{1}{v^n} \frac{\Gamma(n+v, vq_0/\bar{q})}{\Gamma(v)}, \tag{7}$$

where $\Gamma(a, b)$ is the incomplete Euler gamma function. As is true for clouds with vertical inhomogeneity alone, a distribution-based scheme may provide finite values of process rates when single-valued schemes indicate no contribution.

3.3. Linking Vertical and Horizontal Variability

Imagine next a model grid cell in which the vertical gradient of q is constant but optical thickness is distributed horizontally. We must now make a further assumption, since variations in τ might be caused by variations in either drop concentration N or cloud geometrical thickness h. We assume here that N is constant and h varies within the grid cell. This implies that drop size r at each height z within the cloud varies as $r \sim z^{1/3}$. Optical thickness is related to the vertically integrated drop cross section, so $\tau \sim h^{5/3}$.

The PDF of cloud thickness $P(h)$ is related to $P(\tau)$ through $P(\tau)d\tau = P(h)dh$. If $P(\tau)$ follows (3) then

$$P(h) = P(\tau)\frac{d\tau}{dh}$$
$$= C_1 h^{\frac{5v}{3}-1} \exp(-C_2 h^{5/3}), \tag{8}$$

where C_1 and C_2 depend on v, N, β, and $\bar{\tau}$. Finally, the PDF of q can be determined from (8). As in clouds with vertical variability alone, $P(q;h) = 1/\beta h$ for each value of $q \le \beta h$. If we account for all values of h,

$$P(q) = \int_q^\infty \frac{1}{\beta h} P(h) dh$$
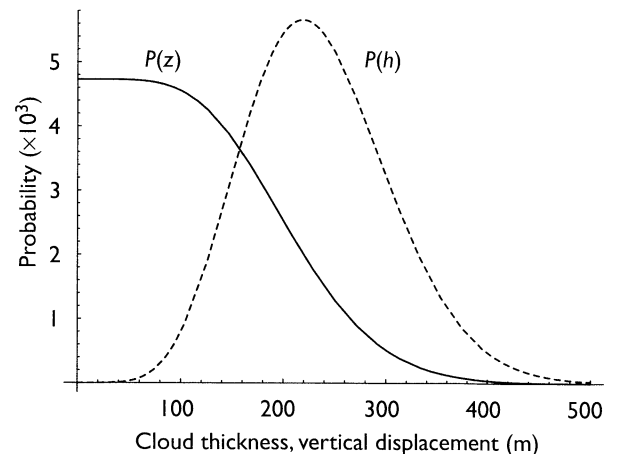$$= C_3 \Gamma(v - 3/5, C_4 q^{5/3}), \tag{9}$$

Figure 2. Probability distributions P of cloud thickness h and vertical displacement from cloud boundary z in a grid cell with constant drop concentration. Changes in cloud thickness cause variability in cloud optical thickness, which is constrained to follow a gamma distribution in accordance with observations. $P(z)$ is linearly related to the distribution of cloud condensate which is used to assess the bias in process rates computed with the average value of q. In this example the mean optical thickness is 10, the standard deviation of τ is half the mean, and the drop concentration $N = 100$ cm^{-3}.
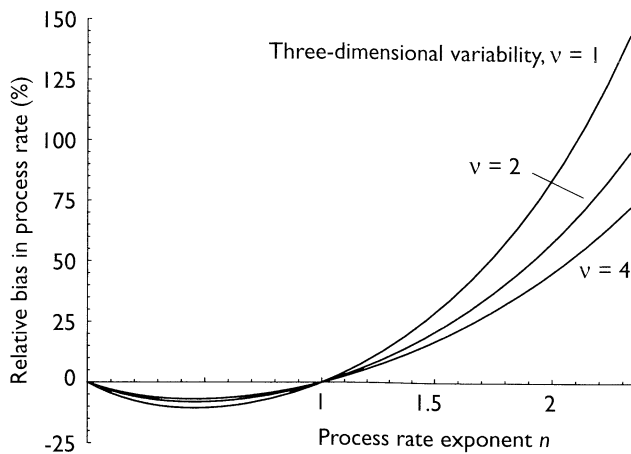
Figure 3. Bias in domain-averaged process rate in the presence of vertical and horizontal variability in q. The distribution $P(q)$ is constructed assuming that optical thickness follows a gamma distribution and that q varies linearly with z. Drop concentration is held constant, so changes in τ are driven by changes in cloud thickness. The bias increases with the amount of variability and the degree of nonlinearity in the process rate. As in Figure 2, the mean optical thickness is 10 and drop concentration $N = 100$ cm^{-3}. Depending on the amount of subgrid-scale variability, the domain-averaged process rate can be more than twice the value computed using the mean value of q.

where C_3 and C_4 again depend on ν, N, β, and $\bar{\tau}$. Consider as an example a cloud with $\bar{\tau} = 10$, $\nu = 4$, $N = 100$ cm^{-3}, which produce the distributions of $P(h)$ and $P(z) = P(q)/\beta$ shown in Figure 2. The great majority of clouds in the grid box are between 100 and 400 m thick. All values of $z < 100$ m are about equally likely, and $P(z)$ has no mode value.

The error in instantaneous process rates is obtained by evaluating (1) with $P(q)$ determined from (9). The resulting integral is not analytically solvable, but the bias can be computed numerically if parameter values are given. Figure 3 shows estimates of the magnitude of the bias for a cloud with mean optical thickness 10 and $N = 100$ cm^{-3} as a function of the degree of nonlinearity n and the amount of variability ν. When the process is strongly nonlinear, process rates computed accounting for the spatial distribution of q can be more than twice the rate computed using the mean value of q alone.

4. Current Practice: Avoiding the SSH Bias by Tuning Model Parameters

Every large-scale model of which we are aware infers grid mean process rates from grid mean values of cloud condensate concentration. We have shown that these process rates are in error by many tens of percent, yet long-term simulations of clouds agree reasonably well with observations. How do models subject to the SSH bias make accurate predictions? The answer lies in the tuning of model parameters.

Cloud schemes in large-scale models have their roots in similar methods developed for finer-scale cloud resolving or mesoscale prediction models. If these schemes are implemented in large-scale models without modification, however, the clouds simulated by the large-scale model are in strong disagreement with observations; in particular, clouds tend to be more reflective and contain more water than observations indicate. Large-scale models are therefore tuned to match observations by adjusting one or more parameter

values. The albedo bias, for example, is typically addressed by reducing the liquid water path used in optical thickness calculations by some arbitrary amount [*Tiedtke*, 1996; *Rotstayn*, 1997]. Liquid water content is very sensitive to the threshold value at which the autoconversion begins [*Rotstayn*, 2000]; this value is usually decreased as the spatial resolution becomes more coarse. These adjustments are made without reference to subgrid-scale inhomogeneity, though unresolved variability is perhaps the most significant reason they are needed.
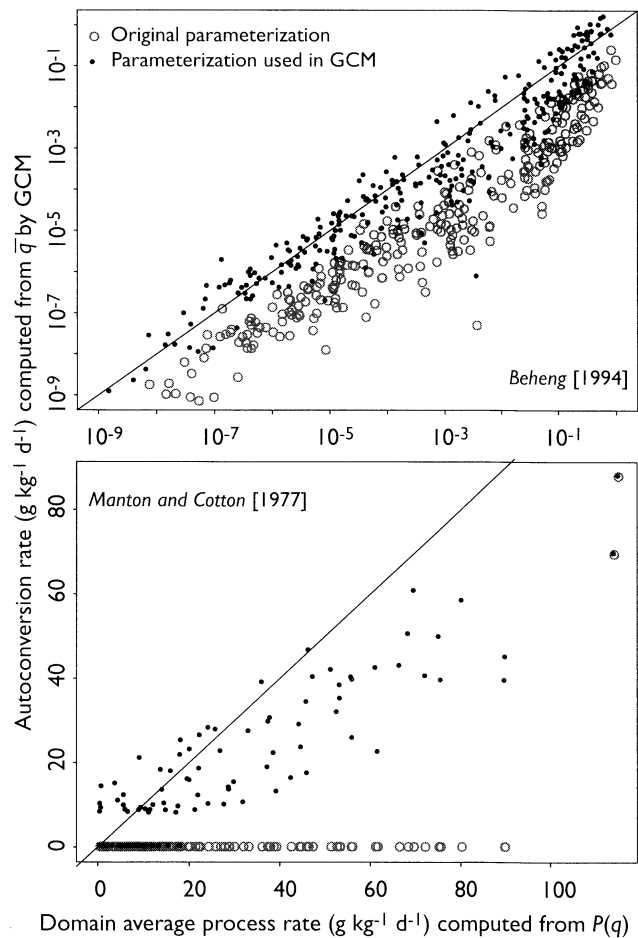

Figure 4. Average autoconversion rates computed from observed subgrid-scale distributions of q by two large-scale model cloud parameterizations. Time-height profiles of q are inferred from cloud radar reflectivity measurements made once a minute in central Oklahoma, and 3-hour average autoconversion rates (shown on the x axis) are compared with rates computed using the average value of q. (top) Autoconversion rate depends on $q^{4.7}$. In all cases the average process rate is substantially higher than the rate computed using original parameterization and a single value of $\bar{q}$ (shown as shaded circles). When implemented in large-scale models this parameterization is tuned by arbitrarily by increasing the rate by a factor of 15 (shown as solid circles). (bottom) Autoconversion is proportional to $q^{7/3}$ once a threshold value of inferred drop radius r_0 is exceeded. Average autoconversion rates computed with $r_0 = 10$ µm vary from 0 to almost 100 g kg^{-1} d^{-1}, but autoconversion rates computed from $\bar{q}$ alone are always zero. The threshold radius must be reduced to 7 µm (or q reduced by a factor of nearly 2) for autoconversion rates to be accurately computed if only the single time average value of q is used. The ad hoc adjustment of model parameters in both examples is made necessary by the neglect of subgrid-scale variability.

We underscore the relationship between spatial variability, average process rates, and parameter adjustment by examining distributions of liquid water content in continental stratiform water clouds. We use 3 months of winter time observations from the millimeter-wavelength cloud radar at the Atmospheric Radiation Measurement Program's Southern Great Plains site in Lamont, Oklahoma. Radar reflectivity values are obtained every 10 s with 45 m vertical resolution. We exclude observations from heavily precipitating clouds and assume a fixed value of $N = 300$ cm^{-3} to relate the radar reflectivity to q. We approximate the distribution of q that would be found within an LSM grid cell centered on the radar location by considering $P(q)$ obtained during each 3-hour interval.

We compute time average autoconversion rates using the parameterization of *Beheng* [1994]. In this formulation, autoconversion depends very strongly on q (as $q^{4.7}$) but occurs at all times (i.e., there is no threshold value). Time average autoconversion rates $\overline{R(q)}$ computed using the original formulation are substantially smaller than $R(\bar{q})$, as shown in the top panel of Figure 4. In fact, the version of this parameterization implemented in a large-scale model [*Lohmann and Roeckner*, 1996] arbitrarily increases the original autoconversion rate by a factor of 15. An SSH bias this dramatic might be expected for this strongly nonlinear process, for example, from modest ($v \approx 2$) horizontal variability alone.

Few parameterizations are as strongly nonlinear, and so as susceptible to the SSH bias, as the Beheng parameterization. The need for tuning is perhaps less for other parameterizations but it can not be avoided. Another commonly used autoconversion parameterization [*Manton and Cotton*, 1977] increases as $q^{7/3}$ once the diagnosed drop radius exceeds a threshold r_0. The parameterization was originally developed for mesoscale models and used a value of roughly $r_0 = 10$ µm; observations suggest a value 2-3 µm larger [*Boers et al.*, 1998]. Three-hour average autoconversion rates $\overline{R(q)}$ computed with $r_0 = 10$ µm range from 0 to about 100 g kg^{-1} d^{-1} (see the bottom panel of Figure 4). When this threshold applied to $\bar{q}$, however, $R(\bar{q})$ is zero for all but a few 3-hour intervals in our sample period because the drop radius diagnosed from $\bar{q}$ is almost always less than 10 µm. The process rate inferred from $\bar{q}$ can be brought into much closer agreement with $\overline{R(q)}$ only if the threshold in the computation of $R(\bar{q})$ is reduced to $r_0 = 7$ µm (a nearly twofold decrease in q_0), as Figure 4 shows. Though the higher threshold value is more realistic (inasmuch as an distinction between cloud and rain water is appropriate in nature), in large-scale models the threshold is typically set to between 5 and 7 µm [*Boucher et al.*, 1995; *Rasch and Kristjánsson*, 1998; *Wilson and Ballard*, 1999]. Figure 4 suggests that subgrid-scale variability is one of the largest factors driving the arbitrary tuning of physical parameterizations in large-scale models.

5. Predicting the Subgrid-Scale Distribution of Water: Statistical Cloud Schemes

In the previous sections we described the SSH bias in the context of prognostic cloud schemes that predict a single mean value of q within each grid cell. The temporal evolution of q is of course coupled in these models to the evolution of water vapor in the domain through source and sink terms. But condensate is just one of the many quantities which vary at the subgrid scale. Water vapor in particular is also quite variable in space and time. Clouds exist where water vapor concentrations reach or exceed saturation, which may occur in some portions of a grid cell but not others. Many large-scale models are tuned to account for the subgrid scale variability of water vapor by introducing a critical relative humidity (usually much less than 100%) at which clouds begin to form.
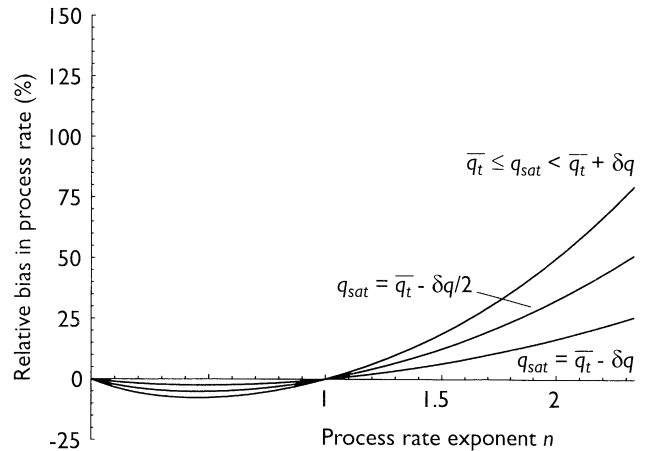

Figure 5. Bias in domain-averaged process rates for a statistical cloud scheme that assumes a triangular distribution with half width δq of total (vapor and condensed) water concentration q_t within each grid cell. The distribution of q, and so the magnitude of the bias, depends on the relationship between the grid cell average total water concentration $\overline{q}_t$ and the saturation concentration q_{sat}. Where $\overline{q}_t < q_{sat}$ the distribution of q is always right triangular and the bias is constant with respect to $q_{sat} - \bar{q}$. As q_{sat} falls below $\overline{q}_t$, however, the distribution becomes more symmetric and the bias decreases. Since statistical cloud schemes make implicit predictions of $P(q)$, these biases could be easily removed from existing models.

One alternative to this aphysical approach is represented by statistical cloud schemes. These algorithms are formulated in terms of the total water content q_t (vapor plus condensate) in each grid cell, which is assumed to be distributed about its mean value $\overline{q}_t$ according to some PDF; popular choices are Gaussian [*Sommeria and Deardorff*, 1977] or triangular [*Smith*, 1990] distributions. Source and sink equations are formulated in terms of q_t. The PDF of q_t, its mean value, and knowledge of the saturation mixing ratio q_{sat} (computed from the mean temperature and pressure) completely define the critical relative humidity, cloud fraction, $\bar{q}$, and $P(q)$ within the grid cell. If $P(q_t)$ is symmetric, then $P(q)$ varies with the relationship between $\overline{q}_t$ and q_{sat}: when $\overline{q}_t < q_{sat}$ the PDF of condensate (if any exists) is skewed toward lower values, with $P(q)$ becoming more and more symmetric as q_{sat} falls below $\overline{q}_t$. In common practice the prognostic equations for q_t are formulated in terms of average condensate amounts, so statistical cloud schemes are also subject to the SSH bias.

We consider as an example the scheme due to *Smith* [1990] which assumes that $P(q_t)$ follows a triangular distribution of half width δq about $\overline{q}_t$. The SSH bias depends on $P(q)$ and so on the relationship between q_{sat} and $\overline{q}_t$. When $\overline{q}_t < q_{sat} < \overline{q}_t + \delta q$, for example, $P(q)$ takes the form of a right triangle where the most frequent value of q is the one closest to 0. In this regime the relationship between $\bar{q}$, and $P(q)$ is constant, so the SSH bias depends only on the amount of nonlinearity in the process rate (see Figure 5). Once q_{sat} falls below $\bar{q}$ the distribution of condensate becomes more symmetric about its mean and the SSH bias decreases, reaching a minimum when $q_{sat} \leq \overline{q}_t - \delta q$.

Statistical cloud schemes as currently formulated are subject to the SSH bias because the source and sink rates are computed from average values of condensate concentration rather than from the average process rate computed from the inferred $P(q)$. Accounting for subgrid-scale variability in such schemes would be straightforward, however.

6. Accounting for Subgrid-Scale Variability in Model Processes

The ad hoc adjustment of model parameters is an evil made necessary by the relatively coarse spatial resolution of climate and weather prediction models. Tuning parameters allows the models to produce fields in agreement with observations but is problematic in theory and in practice. The adjustments are unsatisfying because they lack any concrete physical basis. Furthermore, parameter adjustments are currently uncoupled so that, for example, liquid water path in albedo calculations is reduced without reference to changes made to the autoconversion threshold. Because the amount of unresolved variability changes with model spatial resolution, each parameter has to be readjusted every time a new grid spacing is implemented. Neither is it clear that adjustments made to match current climate are applicable to other regimes.

Explicitly accounting for unresolved spatial variability in q may allow models to make fewer arbitrary adjustments to parameter values. Because the same amount of variability could be included in every process rate computation, the treatment of variability might be incorporated in a consistent manner throughout all the parameterizations in an LSM. The amount of unresolved variability depends in part on the model grid cell spacing, so the rates of all processes will change in concert as model resolution improves.

Several interrelated questions must be addressed if subgrid-scale variability is to be included in large-scale models. Although we have shown a variety of plausible examples, the PDFs of thermodynamic and microphysical properties require much more careful characterization. Are the PDFs easily parameterized in terms of simple distributions? Should different distributions be used in the presence and absence of precipitation? Building up a collection of observed PDFs is a difficult observational task: in section 4, for example, we computed autoconversion rates based on radar observations which fail in the presence of strong precipitation, so our sample is necessarily biased toward light rain. It is also unclear how much of the observed variability is already being resolved; vertical resolution in an LSM and the division of cloud water into convective and stratiform components both account for portions of the total PDF as observed from space. A first step, therefore, is to use a wide variety of sources to describe the unresolved spatial variability in large-scale models.

Progress will also depend on understanding the mechanisms that drive variability and how these may be diagnosed or predicted from information available from the simulation. The subgrid-scale distribution of q reflects the impact of a wide variety of thermodynamic, dynamic, and microphysical processes occurring in each grid cell, and so is a function of season, location, cloud type, and a host of other factors. Even if $P(q)$ is well described by simple few-parameter distributions, large-scale models will still need ways to diagnose or predict the distribution moments. A statistical approach to this problem might use scaling ideas to extrapolate the resolved local variability down to the unresolved subgrid scale [*Cusack et al.*, 1999]. A more physically based method might attempt to relate the amount of variability to the local conditions prevailing in the model. Modifying process rate calculations to account for subgrid-scale inhomogeneity will be straightforward; providing estimates of the amount of variability may prove much more difficult.

Although we have focused on cloud water concentration q, the SSH bias applies to any process rate which depends nonlinearly on a quantity. Accounting for subgrid-scale variations in vertical velocity, for example, can change the ice water path of high stratiform clouds predicted by a large-scale model by a factor of 2 [*Donner et al.*, 1997]. Indeed, since variations in cloud condensate are driven in part by variations in dynamics, it may eventually prove wisest to account for small-scale variability in both dynamical and microphysical processes.

Modifying a large-scale model to account for the effects of subgrid-scale variability would be a significant undertaking, and it is unclear whether simulations of either the mean climate or its sensitivity to perturbation would be affected. Might resources be better spent on, for example, capturing additional physical processes? We believe several compelling reasons exist for pursuing the impact of unresolved variability. First, the sensitivity of some aspects of cloud-aerosol interactions (in particular, the "cloud lifetime indirect effect") are significantly influenced by the details of cloud physical parameterizations [*Lohmann and Feichter*, 1997; *Rotstayn*, 2000]. We also note that while the relative PPH bias in albedo is smaller than the SSH bias in most cases, the PPH bias is considered important enough to include in several large-scale models [*Tiedtke*, 1996; *Rotstayn*, 1997]. Most importantly, all nonlinear processes acting in an LSM are affected by unresolved variability, so parameterizations of additional processes in an LSM will also have to be tuned. We believe it is preferable to explicitly account for the subgrid-scale variability in every process.

References

Barker, H.W., B.A. Wielicki, and L. Parker, A parameterization for computing grid-averaged solar fluxes for inhomogeneous marine boundary layer clouds, II, Validation using satellite data, *J. Atmos. Sci.*, *53*, 2304-2316, 1996.

Beheng, K.D., A parameterization of warm rain cloud microphysical processes, *Atmos. Res.*, *33*, 193-206, 1994.

Boers, R., J.B. Jensen, and P.B. Krummel, Microphysical and short-wave radiative structure of stratocumulus clouds over the Southern Ocean: Summer results and seasonal differences, *Q. J. R. Meteorol. Soc.*, *124*, 151-168, 1998.

Boucher, O., H. Letreut, and M.B. Baker, Precipitation and radiation modeling in a general circulation model: Introduction of cloud microphysical processes, *J. Geophys. Res.*, *100*, 16395-16414, 1995.

Cahalan, R.F., W. Ridgway, W.J. Wiscombe, T.L. Bell, and J.B. Snider, The albedo of fractal stratocumulus clouds, *J. Atmos. Sci.*, *51*, 2434-2455, 1994.

Considine, G., J.A. Curry, and B. Wielicki, Modeling cloud fraction and horizontal variability in marine boundary layer clouds, *J. Geophys. Res.*, *102*, 13,517-13,525, 1997.

Cusack, S., J.M. Edwards, and R. Kershaw, Estimating the subgrid variance of saturation, and its parametrization for use in a GCM cloud scheme, *Q. J. R. Meteorol. Soc.*, *125*, 3057-3076, 1999.

Davis, A.B., A. Marshak, H. Gerber, and W.J. Wiscombe, Horizontal structure of marine boundary layer clouds from centimeter to kilometer scales, *J. Geophys. Res.*, *104*, 6123-6144, 1999.

Del Genio, A.D., M.-S. Yao, W. Kovari, and K.K.W. Lo, A prognostic cloud water parameterization for global climate models, *J. Clim.*, *9*, 270-304, 1996.

Donner, L.J., C.J. Seman, B.J. Soden, R.S. Hemler, J.C. Warren, J. Strom, and K.N. Liou, Large-scale ice clouds in the GFDL SKYHI general circulation model, *J. Geophys. Res.*, *102*, 21,745-21,768, 1997.

Fowler, L.D., D.A. Randall, and S.A. Rutledge, Liquid and ice cloud microphysics in the CSU general circulation model. I. Model description and simulated microphysical processes, *J. Clim.*, *9*, 489-529, 1996.

Khairoutdinov, M., and Y. Kogan, A new cloud physics parameterization in a large-eddy simulation model of marine stratocumulus, *Mon. Weather Rev.*, *128*, 229-243, 2000.

Lohmann, U., and E. Roeckner, Design and performance of a new cloud microphysics scheme developed for the ECHAM general circulation model, *Clim. Dyn.*, *12*, 557-572, 1996.

Lohmann, U., and J. Feichter, Impact of sulfate aerosols on albedo and lifetime of clouds: A sensitivity study with the ECHAM4 GCM, *J. Geophys. Res.*, *102*, 13685-13700, 1997.

Manton, M.J., and W.R. Cotton, Formulation of approximate equations for

modeling moist deep convection on the mesoscale, Atmos. Sci. Pap. 266, Colo. State Univ., Fort Collins, 1977.

Pincus, R., S.A. McFarlane, and S.A. Klein, Albedo bias and the horizontal variability of clouds in subtropical marine boundary layers: Observations from ships and satellites, *J. Geophys. Res., 104*, 6183-6191, 1999.

Rasch, P.J., and J.E. Kristjánsson, A comparison of the CCM3 model climate using diagnosed and predicted condensate parameterizations, *J. Clim., 11*, 1587-1614, 1998.

Rotstayn, L.D., A physically based scheme for the treatment of stratiform clouds and precipitation in large-scale models, *Q. J. R. Meteorol. Soc., 123*, 1227-1282, 1997.

Rotstayn, L.D., On the "tuning" of autoconversion parameterizations in climate models, *J. Geophys. Res., 105*, 15495-15507, 2000.

Smith, R.N.B., A scheme for predicting layer clouds and their water content in a general circulation model, *Q. J. R. Meteorol. Soc., 116*, 435-460, 1990.

Sommeria, G., and J.W. Deardorff, Subgrid-scale condensation in models of non-precipitating clouds, *J. Atmos. Sci.34*, 344-355, 1977.

Sundquist, H., A parametrization scheme for non-convective condensation including prediction of cloud water amount, *Q. J. R. Meteorol. Soc., 104*, 677-690, 1978.

Tiedtke, M., Representation of clouds in large-scale models, *Mon. Weather Rev., 121*, 3041-3061, 1993.

Tiedtke, M, An extension of cloud-radiation parameterization in the ECMWF model: The representation of subgrid-scale variations of optical depth, *Mon. Weather Rev., 124*, 745-750, 1996.

Tjemkes, S.A., and M. Visser, Horizontal variability of temperature, specific-humidity, and cloud liquid water as derived from spaceborne observations, *J. Geophys. Res., 99*, 23089-23105, 1994.

Wilson, D.R., and S.P. Ballard, A microphysically based precipitation scheme for the UK Meteorological Office Unified Model, *Q. J. R. Meteorol. Soc., 125*, 1607-1636, 1999.

S. A. Klein, NOAA Geophysical Fluid Dynamics Laboratory, Princeton University, Princeton, NJ, 08542. (sak@gfdl.gov)

R. Pincus, Cooperative Institute for Meteorological Satellite Studies, University of Wisconsin, 1225 W. Dayton St., Madison, WI 53706. (Robert.Pincus@ssec.wisc.edu)